American Mineralogist, Volume 80, pages 585–592, 1995

# Exsolution lamellae of kirschsteinite in magnesium-iron olivine from an angrite meteorite

TAKASHI MIKOUCHI, HIROSHI TAKEDA, MASAMICHI MIYAMOTO
Mineralogical Institute, Graduate School of Science, University of Tokyo, Hongo, Tokyo 113, Japan
KAZUMASA OHSUMI
Photon Factory, National Laboratory for High Energy Physics (KEK), Tsukuba, Ibaraki 305, Japan
GORDON A. MCKAY
SN4 NASA/Johnson Space Center, Houston, Texas 77058, U.S.A.

## ABSTRACT

Exsolution phenomena of kirschsteinite ($CaFeSiO_4$) in olivine have been studied by single-crystal X-ray diffraction techniques and scanning electron microscopy (SEM) of oriented polished thin sections (PTS) of three single crystals separated from the Antarctic angrite LEW86010, supplemented by micro-area X-ray diffraction with the Laue method (MXL) by synchrotron radiation (SR) for PTS of a rock chip of LEW86010. The cell dimensions of the host olivine and exsolved kirschsteinite are $a$ = 4.79(3), $b$ = 10.39(5), and $c$ = 6.06(3) Å, and $a$ = 4.87(5), $b$ = 11.14(10), and $c$ = 6.36(5) Å, respectively, from the precession photos. The PTS of olivine single crystals oriented parallel to (100) show exsolution lamellae of kirschsteinite up to 10 $\mu$m in width. The two sets of lamellae are symmetrically related and parallel to (031) and ($0\bar{3}1$). Electron microprobe analysis gave $SiO_2$ 33.1, $TiO_2$ 0.07, $Al_2O_3$ 0.03, FeO 49.4, MnO 0.61, MgO 13.4, CaO 2.2, $Cr_2O_3$ 0.02, $V_2O_3$ 0.01, NiO 0.05 (sum 99.4 wt%) for the host olivine and $SiO_2$ 33.3, $TiO_2$ 0.03, FeO 31.5, MnO 0.39, MgO 5.4, CaO 28.5, $Cr_2O_3$ 0.02, NiO 0.05 (sum 99.2 wt%) for the exsolved kirschsteinite. The results from MXL for the olivine crystals on the rock PTS are compatible with the observation on the single crystals that the lamellae are parallel to (031) and ($0\bar{3}1$). The (031) and ($0\bar{3}1$) planes have been known to be twin planes for olivine, and the twinning is by reticular pseudomerohedry based on a quadruple lattice. Although other reported exsolved precipitates in meteoritic olivines exist as inclusions, kirschsteinite in LEW86010 olivine takes the form of lamellae. Our explanation is that LEW86010 olivine is Fe-rich and that lamellar precipitates are more easily formed than inclusions because exsolution lamellae along {031} in Fe-rich olivine maintain lattice coherency.

## INTRODUCTION

Exsolution textures are frequently observed in minerals of igneous and metamorphic rocks and often take the form of lamellar precipitates. Exsolution occurs when an originally homogeneous phase enters a two-phase field, usually as a result of reduction in temperature. The growth of an exsolved phase causes a redistribution of elements, which can give some information on the cooling history. These exsolution textures are commonly observed in plagioclases, pyroxenes, amphiboles, and other rock-forming minerals (Putnis, 1992). The exsolution of Ni-Fe metal in Fe meteorites is well known (Widmanstätten pattern), and Goldstein and Short (1967) calculated the cooling rates of these meteorites assuming the Ni-rich lamellae were formed by diffusion. Miyamoto and Takeda (1994) calculated the thickness of the crust of HED (horwardite, eucrite, diogenite) parent body from augite lamellae in pigeonite host crystals in a cumulate eucrite (Moore County). Although olivine is one of the most important rock-forming minerals and is common in both terrestrial and extraterrestrial materials, exsolution phenomena in olivine have not been well characterized. Ashworth (1979) found two kinds of exsolution of chromite in chondritic olivine. Petaev and Brearley (1994) and Petaev et al. (1994) reported a lamella-like texture produced in the olivine in the Divnoe achondrite. Dodd (1971) identified ferroan monticellite (kirschsteinite) insets in chondritic olivine, but they are not lamellae. Prinz et al. (1977) reported kirschsteinite inclusions in the Angra dos Reis achondrite. Prior to the recovery of LEW86010 Antarctic angrite, the presence of forsterite lamellae in a monticellite host ($CaMgSiO_4$) was the only instance of exsolution lamellae in olivine ever reported (Willemse and Bensch, 1964; Tracy et al., 1978).

Angrite are unusual meteorites, of which the first sample discovered was Angra dos Reis. Angrites are basaltic achondrites with fassaite, olivine, and anorthite. In the last eight years three additional angrites were recovered from Antarctica (Mason, 1987, 1989; Yanai, 1991). Angrites are noted for their very old crystallization ages (4.55 b.y.) and are said to be one of the oldest known basalts

0003–004X/95/0506–0585$02.00

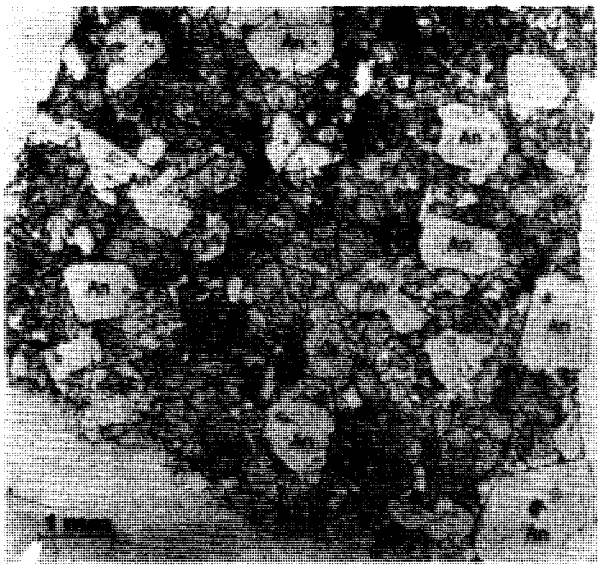

Fig. 1. Optical photomicrograph of LEW86010 thin section (LEW86010,6) (parallel polarized light). Zoned fassaite (Fs), olivine with kirschsteinite lamellae (Ol), and anorthite (An) are major constituent minerals. Kirschsteinite lamellae occur in two orientations. The scale bar is 1 mm.

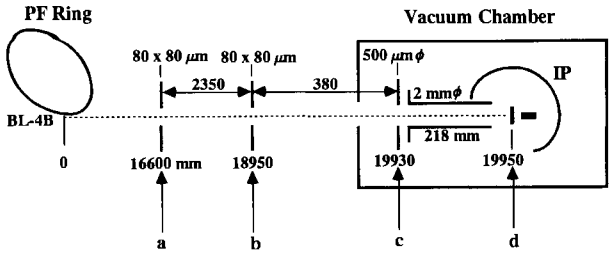


Fig. 2. A schematic illustration of the optical system and diffraction equipment of MXL. PF ring is a storage ring for SR experiments. Letters a, b, and c indicate the first and second slit and third pinhold, respectively. Sample (thin section) and imaging plate are indicated by d and IP, respectively. The numbers situated below the horizontal dotted line are the distances from the source point (o).

in the solar system (Lugmair and Galer, 1992). One of the most remarkable characteristics of angrites is that they are conspicuously rich in refractory elements and poor in volatile elements. The origins of the angrite are still under dispute (Mittlefehldt et al., 1990).

LEW86010, discovered in Antarctica in 1986, is the second angrite to be identified (Mason, 1987). Olivine with a high bulk Ca content is one of the major constituent minerals of LEW86010, and it exsolved kirschsteinite (ideally $CaFeSiO_4$) during cooling (McKay et al., 1988; Goodrich, 1988; Prinz et al., 1988; Delaney and Sutton, 1988).

Although Mason (1987) first described kirschsteinite lamellae in the LEW86010 olivine, and Prinz et al. (1988) and McKay et al. (1989) described the lamella directions on nonoriented PTS of a rock chip, this report and our preliminary one (Mikouchi et al., 1993) represent the first crystallographic study of the relationship between the host and the lamellae. This exsolution texture is the only case known in which kirschsteinite lamellae formed in a Ca-poor olivine (fayalite) host, as is commonly observed in pyroxenes. The coexistence of olivine and exsolved phases provides us with information on the phase relations between Ca-poor and Ca-rich olivine (Davidson and Mukhopadhyay, 1984), and its cooling history can be deduced by the method applied to other minerals (Goldstein and Short, 1967; Miyamoto and Takeda, 1994). Employing Ca diffusion profiles of kirschsteinite in this angrite olivine, McKay et al. (1989, 1993) estimated a cooling rate for this meteorite.

Although kirschsteinite was recently found in a carbonaceous chondrite (Kimura and Ikeda, 1994), it is extremely rare on the Earth and is known to be produced in only a few places in the world (Sahama and Hytönen, 1957, 1958; Konev et al., 1970). Magnesian kirschsteinite, reported by Sahama and Hytönen (1957), occurs in a melilite nephelinite, North Kivu, Zaire, in which it is associated with kalsilite, götzenite, sodalite, combeite, and perovskite. Magnesium kirschsteinite has also been described from calcareous skarn xenoliths in the alkali syenite, Tazheran, Russia (Konev et al., 1970).

We examined the exsolution lamellae of kirschsteinite in oriented olivine single crystals from the LEW86010 angrite using X-ray diffraction, optical microscopy, SEM, and electron microprobe analysis. Because the crystallographic orientation of kirschsteinite lamellae obtained by oriented single crystals is different from that determined by optical microscope observation of the PTS (Prinz et al., 1988; McKay et al., 1989), olivines in the LEW86010 PTS were analyzed by micro-area X-ray diffraction with the Laue method (MXL) developed by Ohsumi et al. (1991, 1993) using synchrotron radiation (SR) at beam line 4B (BL-4B) of the Photon Factory (PF), National Laboratory for High Energy Physics (KEK) in Tsukuba, Japan. The lamella directions determined by MXL were compared with the results of oriented single crystals. This new technique allows in-situ crystallographic microanalysis of minerals in thin section at spatial resolutions comparable with the electron microprobe.

## Samples and experimental methods

### Sample description

Antarctic angrite LEW86010 weighs only 6.9 g (Mason, 1987) and has approximate dimensions of 1.5 cm on each side. Five olivine grains separated from LEW86010,10,14 by L. E. Nyquist and coworkers (NASA Johnson Space Center), were used for this study as a part of the consortium study led by G. McKay. Each grain is about 0.5 mm in diameter and, when viewed through an optical microscope, appears to be a yellowish single crystal. Only three

of the crystals were used for this study, and the rest were kept for a future study.

In addition to three single crystals, a polished thin section of a rock chip (PTS LEW86010,6) (Fig. 1) was examined by MXL at the PF, at KEK in Tsukuba, Japan. The modal abundances of minerals in this PTS are 43.3% pyoxene, 31.8% plagioclase, 20.3% olivine, 3.2% kirschsteinite, 0.7% troilite, 0.3% whitlockite, and 0.1% hercynite (McKay et al., 1988). Olivine occurs as subhedral to anhedral crystals. All olivines show exsolution lamellae of kirschsteinite, which are mostly parallel to two crystallographic directions.

### Single-crystal X-ray diffraction

For determination of the crystallographic orientation of the olivine grains, a single-crystal X-ray diffraction technique (precession camera) was employed, using Ni-filtered Cu$K\alpha$ ($\lambda$ = 1.5418 Å) and Zr-filtered Mo$K\alpha$ ($\lambda$ = 0.7107 Å) radiation. At first, each grain was carefully mounted on a glass fiber using oxybenzon. The $(hk0)^*$ and $(h0l)^*$ reciprocal nets were photographed by a precession camera with a 0.1-mm slit. Exposure times were 50–120 h at 40 kV, 15 mA. The cell dimensions of the host olivine phases were calculated from the distances between the pair of reciprocal lattice rows measured on the photographs by a comparator. After the orientation of the host olivine was defined, other reflections that do not belong to the host were searched for, and a match was sought with reflections from exsolved kirschsteinite. Then, the grain was mounted in resin with its crystallographic $a$ axis perpendicular to the plane of the glass slide, since the reported lamella directions were all parallel to the $a$ axis (Prinz et al., 1988; McKay et al., 1989). The crystal was polished parallel to the (100) plane, which is perpendicular to the lamella planes. The depth of polishing was controlled to get the widest cross section. Crystallographic orientations of the lamellae were determined with respect to the crystallographic $b$ and $c$ axes of the host, as determined by the precession method. The width of the exsolution lamellae and the spacings between them were measured through an optical microscope. After C coating, the grain was observed by a JEOL JSM-840 SEM equipped with an energy-dispersive X-ray spectrometer (EDS). The chemical composition of kirschsteinite exsolution lamellae and host olivine were obtained with the JEOL Super Probe 733 at the Ocean Research Institute of the University of Tokyo with a 12-nA beam current and 15-kV accelerating voltage.

### Microdiffraction on a thin section by synchrotron radiation

The olivine crystals in the PTS of LEW86010 were analyzed by SR at BL-4B of the PF. The Laue method (MXL) was used to record the diffraction patterns with an imaging plate (Ohsumi et al., 1991). Although this measurement yielded a minimum beam diameter of 8 $\mu$m, a beam diameter of about 50 $\mu$m was used for the MXL measurement to cover both the lamella and the host. The Laue patterns of the LEW86010 olivines were taken with 10-min exposures, with the storage ring current at around 250 mA and a ring energy at 2.5 GeV. A computer software system developed for analysis of micrometer-sized single crystals (Hagiya et al., 1993) has been revised and used for data reduction. A schematic illustration of this entire system is shown in Figure 2, and a detailed description of the method is given by Ohsumi et al. (1994).

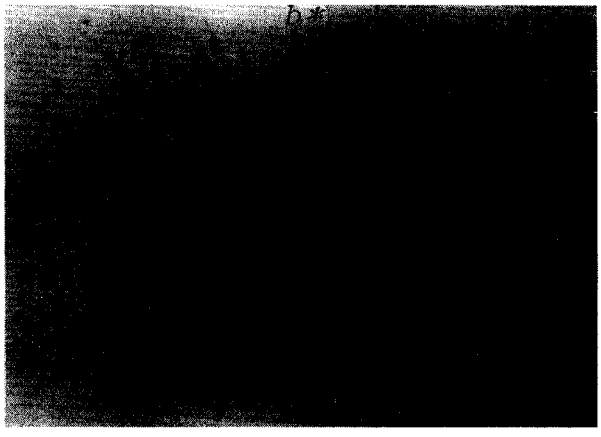

Fig. 3. X-ray diffraction photos of $(hk0)^*$ and $(h0l)^*$ planes by precession camera. Faint reflections from kirschsteinite are observed just inside those from the host olivine. The intense kirschsteinite reflections correspond to the reflective powder diffraction intensities for kirschsteinite.

The orientation of the sample with respect to the coordinate system of the equipment is calculated based on the positions of the Laue spots on the imaging plate using indices and cell dimensions of olivine obtained from the precession method. We calculated the angles between the two sets of lamellae that would be observed in the plane of the PTS, assuming that the lamellae are parallel to (031) and $(0\bar{3}1)$, and compared the calculated angles with those actually observed on the PTS.

## Results

### Crystallographic data

**Host olivine.** The olivine in the forsterite-fayalite solid-solution series is orthorhombic with space group *Pbnm*. Kirschsteinite belongs to the same crystal system and space group as olivine. The cell dimensions were measured on the precession photographs taken with Cu$K\alpha$ radiation. These sets of $a$, $b$, and $c$ axis precession photographs give the cell dimensions of the host olivine as $a$ = 4.79(3), $b$ = 10.39(5), and $c$ = 6.06(3) Å by refinement of about 50 pairs of reciprocal lattice rows (Fig. 3). Using a diagram of cell dimensions vs. Mg/(Mg + Fe) atomic ratios for the forsterite-fayalite solid-solution series (Akimoto, 1976; Hazen, 1977), the Mg/(Mg + Fe) atomic ratio of approximately 0.3 ($Fo_{30}$) is obtained for the above cell dimensions without taking the Ca content into ac-

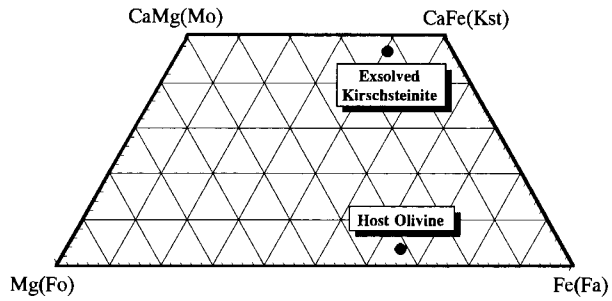


Fig. 4. Chemical composition (in mole percent) of exsolved kirschsteinite and host olivine plotted in the calcium-magnesium-iron olivine quadrilateral.

**TABLE 1.** Electron microprobe analysis (in weight percent) of the host olivine and exsolved kirschsteinite in angrite LEW86010

| | Host olivine | Kirschsteinite lamella |
|---|---|---|
| $SiO_2$ | 33.1 | 33.3 |
| $TiO_2$ | 0.07 | 0.03 |
| $Al_2O_3$ | 0.03 | — |
| FeO | 49.4 | 31.5 |
| MnO | 0.61 | 0.39 |
| MgO | 13.4 | 5.4 |
| CaO | 2.2 | 28.5 |
| $Na_2O$ | — | 0.01 |
| $K_2O$ | — | — |
| $Cr_2O_3$ | 0.02 | 0.02 |
| $V_2O_3$ | 0.01 | — |
| NiO | 0.05 | 0.05 |
| $P_2O_5$ | — | — |
| Total | 99.4 | 99.2 |

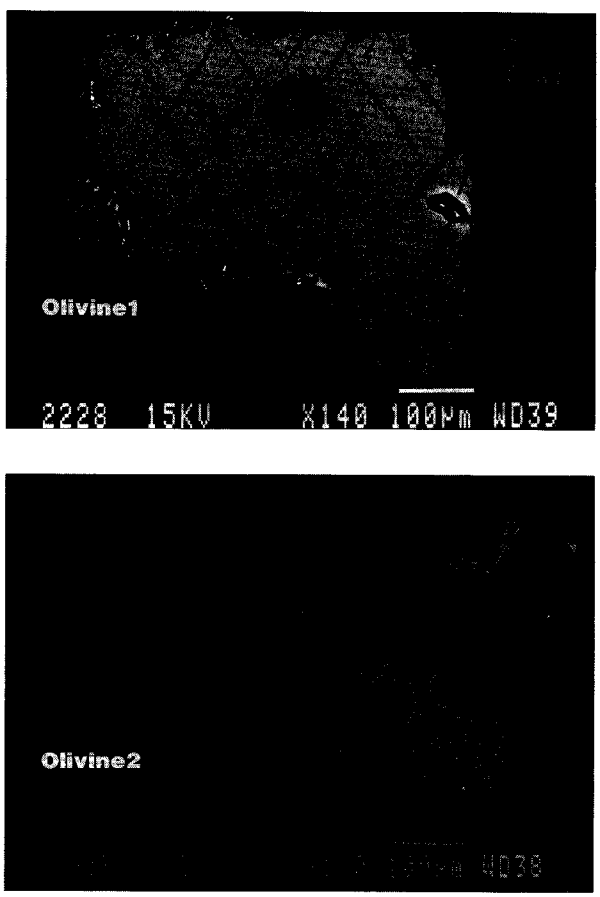


Fig. 5. Back-scattered electron (BSE) images of two oriented olivine crystals (Olivine1 and Olivine2). Both olivine grains include exsolution lamellae of kirschsteinite parallel to (031) and ($0\bar{3}1$). The thickness of the lamellae is at most 10 $\mu$m and the spacing is generally several tens of micrometers. The black spherical mineral in Olivine1 is anorthite. Exsolved precipitates are observed at the crystal boundary. Several black lines crossing the lamellae are the traces of microprobe analysis. An: anorthite, Ol: host olivine, and Kst: kirschsteinite lamella.

count. This ratio is in relatively good agreement with the values ($Fo_{32}$) later obtained by microprobe analysis as well as previously reported values ($Fo_{31-33}$) (McKay et al., 1988; Delaney and Sutton, 1988; Prinz et al., 1988; Goodrich, 1988). Chemical compositions of the host olivine and the exsolved kirschsteinite are listed in Table 1, and Ca-Fe-Mg atomic ratios are plotted on the olivine quadrilateral (Fig. 4).

**Exsolved phase.** The faint reflections just inside the host olivine reflections were recognized on the ($hk0$)* and ($h0l$)* photographs (Fig. 3). Generally, the higher the Fe content of olivine, the greater the absorption of X-rays. These olivines have high Fe contents ($Fo_{32}$). As a result, the exsolved phase was easier to detect on the photos taken with Mo$K\alpha$ radiation than on those with Cu$K\alpha$ because of the weaker absorption of Mo$K\alpha$ X-rays. Because the exsolved and the host phases have the same crystallographic orientations, we can obtain the cell dimensions of the exsolved phase as $a$ = 4.87(5), $b$ = 11.14(10), and $c$ = 6.36(5) Å, which are in close agreement with the reported cell dimensions for kirschsteinite (Sahama and Hytönen, 1958). Furthermore, the indices of intense reflections found among the list of the intense reflections in the powder diffraction file reported for kirschsteinite are also intense on the precession photos (Sahama and Hytönen, 1958) (Table 2).

### Orientation of the exsolution lamellae

Examination by an optical microscope and SEM revealed that all olivine crystals polished parallel to (100) contain two sets of distinct exsolution lamellae up to 10 $\mu$m in width and perpendicular to (100) (Fig. 5). Spacings between the lamellae are typically a few tens of micrometers. The lamellae looked perpendicular to the observed plane (100). The observed angles between the two lamella directions were all about 58–65°. The two sets of lamellae are symmetrically related with respect to the crystallographic $b$ and $c$ axes. The lamellae position did not move while the sections were polished. All those results indicate that the lamellae are parallel to the $a$ axis.

There is good agreement between the observed angle

**TABLE 2.** X-ray crystallographic data for kirschsteinite*

| Kirschsteinite $CaFeSiO_4$ | | |
|---|---|---|
| $d$ (Å) | $I/I_1$ | $hkl$ |
| 5.58 | 50 | 020 |
| 4.22 | 35 | 021 |
| 3.895 | 5 | 101 |
| 3.672 | 60 | 111 |
| 2.957 | 100 | 130 |
| 2.788 | 30 | 040 |
| 2.687 | 90 | 131 |
| 2.612 | 95 | 112 |
| 2.559 | 20 | 041 |
| 2.421 | 35 | 140 |
| | | 122 |
| 2.176 | 10 | 132 |
| 1.835 | 60 | 240 |
| | | 222 |
| 1.610 | 35 | 062 |
| | | 004 |

*Note:* system = orthorhombic; space group = *Pbnm*; $a$ = 4.875, $b$ = 11.155, $c$ = 6.438 Å.
* From Sahama and Hytönen (1958).


Fig. 6. Optical photomicrograph of an olivine crystal in PTS LEW86010,6. The angle between the two sets of lamellae is 60°. An: anorthite; Ol: olivine.

between the lamellae (58–65°) and the angle between (031) and (0$\bar{3}$1) (59.6°), calculated using the observed host-olivine cell dimensions. The agreement indicates that the lamellae are indeed parallel to (031) and (0$\bar{3}$1). The difference between the observed and calculated angles are within error because the plane of observation may not be exactly parallel to (100). Table 3 shows that other potential orientations do not show similar agreement.

Although we cannot detect the textural relationship between the lamellae and the host from only the diffraction images taken with the Laue method (MXL) by SR, those images provide information on the crystallographic directions of the crystals in the X-ray beam. Using the orientation matrix obtained by MXL for the olivine in the PTS, and assuming the lamella directions, we can calculate the lamella angle on the plane of the PTS and compare it with the observed angle.

One olivine grain on the LEW86010 PTS shows that the angle between the two lamellae is about 60° (Fig. 6). The orientation matrix from the MXL is $rx$: −171.3, $ry$: −65.26, and $rz$: 128.65°. If the lamellae are assumed to be parallel to (031) and (0$\bar{3}$1), the lamellae angle is calculated to be 61° on the PTS. This angle is in good agreement with the observed values for the crystal (Table 4).

## DISCUSSION

Our results indicating lamellae parallel to (031) and (0$\bar{3}$1) do not agree with the previously reported orientation parallel to (011) and (0$\bar{1}$1) (McKay et al., 1989), or to (001) and (011), or to (001) and (031) (Prinz et al., 1988). Each angle between a set of two directions is roughly 60°, except for (001) and (011) pairs (Fig. 7). The width of the lamellae previously reported is about 15–20 μm, which is wider than the values of this study (up to 10 μm), indicating that the kirschsteinite lamellae of the previous study are not exactly perpendicular to the plane of the PTS. One possible explanation of these differences is that the previous thicknesses were measured on non-oriented thin sections, for which the lamellae tend to give larger values, and the researchers might have mistaken their crystallographic axes. There is also a possibility that their crystallographic axes might have been rotated 60° under microscopic observation. For example, if the $b$ axis is exchanged with the $c$ axis, (011) and (0$\bar{1}$1) nearly agree with (031) and (0$\bar{3}$1). Furthermore, if the (0$kl$) plane (including $b$ and $c$ axes) is rotated by 60°, the (001) and (031) pair are also in good agreement with (031) and (0$\bar{3}$1).

MXL also indicated that the result from the oriented section is consistent with the lamellae being parallel to (031) and (0$\bar{3}$1). We cannot exclude the possibility that lamellae of several directions may truly exist. However, a consideration of the atomic structure of olivine suggests that the planes parallel to (031) and (0$\bar{3}$1) are stable directions for lamellae, as is discussed later.

**TABLE 3.** Calculated angles* between two lamellae using cell dimensions of the observed olivine

| Lamellae | Angle (°) |
|---|---|
| ∥(011) and (0$\bar{1}$1) | 119.5 |
| ∥(021) and (0$\bar{2}$1) | 81.2 |
| ∥(031) and (0$\bar{3}$1) | 59.5 |
| ∥(041) and (0$\bar{4}$1) | 46.4 |

* The observed angles between two lamellae are 58–65°.

**TABLE 4.** Calculated angles* between two lamellae observed on the PTS using the data from SR analysis

| Lamellae | Angle (°) |
|---|---|
| ∥(001) and (011) | 28 |
| ∥(001) and (031) | 55 |
| ∥(011) and (0$\bar{1}$1) | 88 |
| ∥(031) and (0$\bar{3}$1) | 61 |

* The observed angle between two lamellae on the section is 60°.

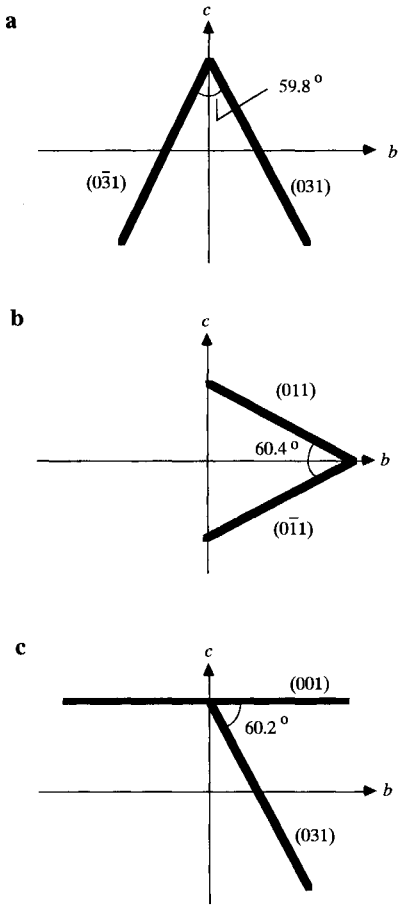


Fig. 7. Schematic illustrations of the lamellae directions reported by previous workers and comparison with this work. (**a**) This work [parallel to (031) and (0$\bar{3}$1)], (**b**) McKay et al., 1989 [parallel to (011) and (0$\bar{1}$1)], and (**c**) Prinz et al., 1988 [parallel to (001) and (031)]. All reports indicate that the angles between the two sets of lamellae are nearly 60°.

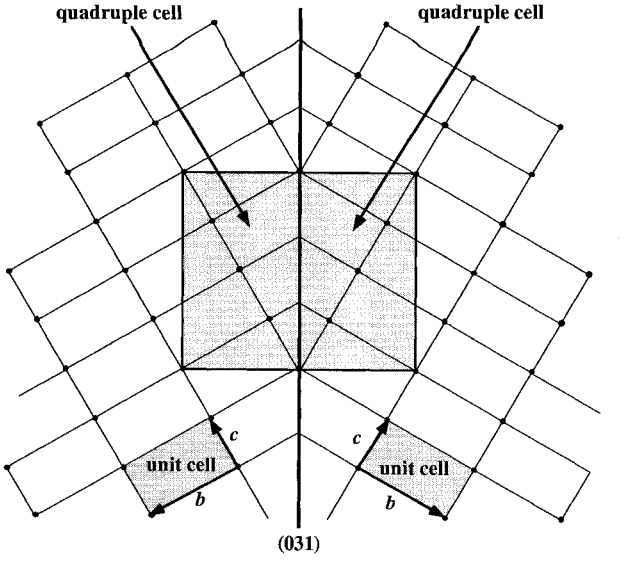


Fig. 9. Schematic illustration of olivine cells with the twin plane of (031). The (031) plane defines a quadruple lattice for twinning by reticular pseudomerohedry because the ratio of the cell dimension of the *b* axis and *c* axis is almost the square root of 3:1.

Figure 8 depicts the crystal structure within a unit cell of forsterite perpendicular to the *a* axis (Bragg and Brown, 1926). The plane of dense O distribution is parallel to the (031) and (0$\bar{3}$1) planes. Twinning in monticellite is not common, but {031} are known to be twin planes (Larsen et al., 1941) and olivine also has twinning on (031). Figure 9 shows a schematic illustration of a larger scale with twin plane of (031). The quadruple lattice can be taken for a twinning by pseudomerohedry, because the ratio of the cell dimension of the *b* axis and *c* axis is almost the square root of 3:1.

Exsolved precipitates in Angra dos Reis and Sharps chondrite do not take the form of lamellae, but they exist as inclusions (Prinz et al., 1977; Dodd, 1971). Taking the cell dimensions of the *b* and *c* axes of olivine at various Fo contents (Hazen, 1977), we calculated the *b*/*c* ratios and the angles ($\theta$) (tan $\theta$ = *b*/*c*). The cell dimensions at 1000 °C were employed because the exsolution was estimated to occur at this temperature (Davidson and Mukhopadhyay, 1984). As the Fa content increases, the $\theta$ value also increases and approaches 60° (Fig. 10), at which point the ideal quadruple cell can be taken. This result shows that more Fe-rich olivine will give a quadruple cell with smaller twin obliquity (Kasper and Lonsdale, 1972), which also indicates the possibility that exsolution la-

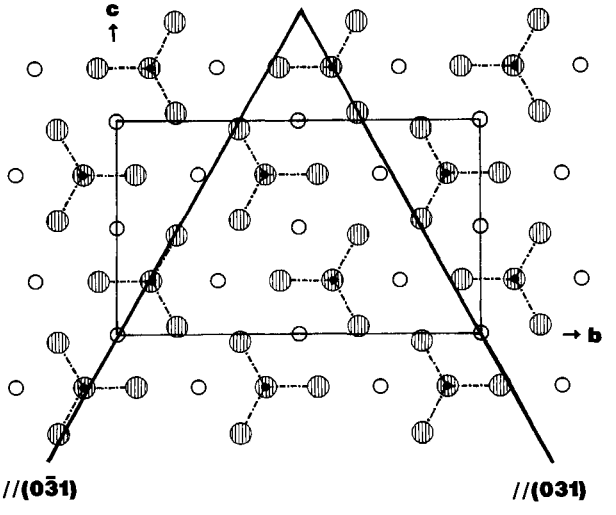


←

Fig. 8. Schematic illustration of the forsterite structure within the unit cell, from the **a** direction. Note the dense plane of O distribution along the {031} plane. The open circles represent Mg, the solid circles represent Si, and the striped circles represent O.

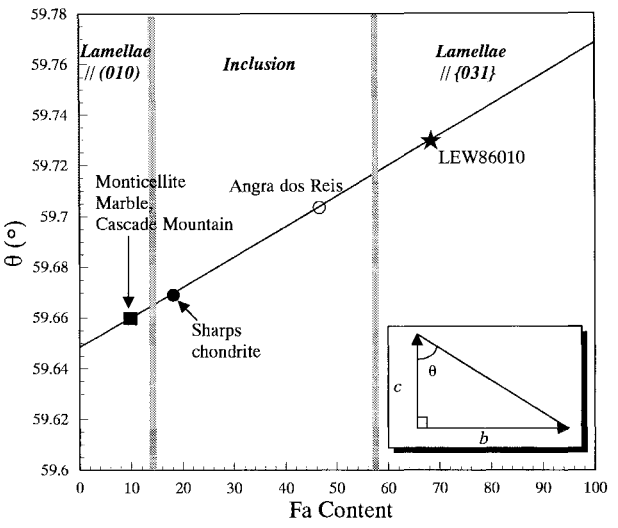


Fig. 10. The relation between Fa content and $\theta$ corresponding to the $b/c$ ratios. This figure indicates that the more Fe-rich olivine can take the quadruple cell with smaller twin obliquity.

mellae along {031} in Fe-rich olivine maintain lattice coherency. This is in line with the natural occurrence of exsolved precipitates. The most Fe-rich olivine ($Fo_{31}$) has exsolution lamellae and the less Fe-rich olivines, Angra dos Reis ($Fe_{53}$) and Sharps chondrite ($FO_{78}$), do not have lamellae, but instead have rounded inclusions of exsolved phases (Prinz et al., 1977; Dodd, 1971). The textural transition boundary between lamella and inclusion may exist around $Fe_{40}$. Forsterite lamellae ($Fo_{90-94}$) parallel to (010) have been reported in a monticellite host (Tracey et al., 1978). In this case we have to consider another mechanism to explain the formation of (010) lamellae in monticellite. We also calculated twin obliquity at room temperature and obtained a similar result. This shows that compositional difference plays a more important role than thermal expansion at high temperature. However, it is difficult to reach a definite conclusion because we have few examples of the exsolution phenomenon of olivine. An experimental study that produces exsolved phases of olivine at various Fo contents is required for further discussion.

Fukuda (1992) calculated the orientation of the invariant plane in belite ($Ca_2SiO_4$) assuming undistorted planes when an initial unit sphere of the originally homogeneous phase is distorted into an ellipsoid of the exsolved phase. The calculated planes are in good accordance with the observed ones. In the case of kirschsteinite lamellae and host olivine in the LEW86010 olivine, the cell dimensions of kirschsteinite are always larger than those of olivine. Thus, we cannot obtain any unique solution by this method.

## Acknowledgments

The Meteorite Working Group generously supplied us with the sample of LEW86010 as part of the consortium study. We thank H. Mori at Ehime University for his technical support for making oriented thin sections. The discussions with the staff of the Mineralogical Institute of the University of Tokyo and K. Fukuda of the Nagoya Institute of Technology were very helpful. We are also indebted to O. Tachikawa and T. Takase of the Mineralogical Institute for their technical assistance, and J. Wagstaff and L. Le of Lockheed/ESCO for their helpful suggestions. We thank the Ocean Research Institute of the University of Tokyo for microprobe analysis. The manuscript benefitted from constructive reviews by J.H. Berg, A. Brearley, and an anonymous reviewer.

## References cited

Akimoto, S., Matsui, Y., and Syono, Y. (1976) High-pressure crystal chemistry of orthosilicates and the formation of the mantle transition zone. In R.G.J. Strens, Ed., The physics and chemistry of minerals and rocks, p. 327–363. Wiley, New York.

Ashworth, J.R. (1979) Two kinds of exsolution in chondritic olivine. Mineralogical Magazine, 43, 535–538.

Bragg, W.L., and Brown, G.B. (1926) Die struktur des olivins. Zeitschrift für Kristallographie, 63, 538–556.

Davidson, P.M., and Mukhopadhyay, D. (1984) Ca-Fe-Mg olivines: Phase relations and solution model. Contributions to Mineralogy and Petrology, 86, 256–263.

Delaney, J.S., and Sutton, S.R. (1988) LEWIS CLIFF 86010, an ADORable Antarctican. Lunar and Planetary Science, XIX, 265–266.

Dodd, R.T. (1971) Calc-aluminous insets in olivine of the Sharps chondrite. Mineralogical Magazine, 38, 451–458.

Fukuda, K. (1992) Intracrystalline microtexture formed by the polymorphic phase transition in belite. Ph.D. thesis, Nagoya Institute of Technology, Nagoya, Japan.

Goldstein, J.I., and Short, J.M. (1967) Cooling rates of 27 iron and stony-iron meteorites. Geochimica et Cosmochimica Acta, 31, 1001–1023.

Goodrich, C.A. (1988) Petrology of the unique achondrite LEW86010. Lunar and Planetary Science, XIX, 399–400.

Hagiya, K., Takase, T., Shimizugawa, Y., Ohsumi, K., Miyamoto, M., and Ohmasa, M. (1993) Software system for microcrystallography with white SR Laue method. Acta Crystallographica, A49, Supplement, 57.

Hazen, R.M. (1977) Effects of temperature and pressure on the crystal structure of ferromagnesian olivine. American Mineralogist, 62, 286–295.

Kasper, J.S., and Lonsdale, K., Eds. (1972) International tables for X-ray crystallography, vol. II, p. 101–150. Kynoch, Birmingham, U.K.

Kimura, M., and Ikeda, Y. (1994) Alkali-lime reactions of Allende chondrule: II. Ca-rich phases in chondrules. Abstract for 19th Symposium on Antarctic Meteorites, 22–23.

Konev, A.A., Ushchapovskaya, Z.F., and Lebedeva, V.S. (1970) First find of magnesian kirschsteinite in the USSR. Døklady Adademie Nauk SSSR, Earth Science Section, 190, 136–138.

Larsen, E.S., Hurlbut, C.S., Buie, B.F., and Burgess, C.H. (1941) Igneous rocks of the Highwood Mountains, Montana VI. Bulletin of Geological Society of America, 52, 1841–1868.

Lugmair, G.W., and Galer, S.J.G. (1992) Age and isotopic relationships among the angrites Lewis Cliff 86010 and Angra dos Reis. Geochimica et Cosmochimica Acta, 56, 1673–1694.

Mason, B. (1987) Antarctic Meteorite Newsletter, 10(2), 32.

——(1989) Antarctic Meteorite Newsletter, 12(1), 15.

McKay, G., Lindstrom, D., Yang, S.-R., and Wagstaff, J. (1988) Petrology of unique achondrite LEWIS CLIFF 86010. Lunar and Planetary Science, XIX, 762–763.

McKay, G., Miyamoto, M., and Takeda, H. (1989) Cooling history of angrite LEW86010 (abs.). Meteoritics, 24, 302.

McKay, G., Ogawa, T., Miyamoto, M., and Takeda, H. (1993) More on the cooling history of angrite LEW 86010. Lunar and Planetary Science, XXIV, 967–968.

Mikouchi, T., Takeda, H., Mori, H., Miyamoto, M., and McKay, G. (1993) Exsolved kirschsteinite in angrite LEW86010 olivine. Lunar and Planetary Science, XXIV, 987–988.

Mittlefehldt, D.W., Lindstrom, M.M., and Lindstrom, D.J. (1990) Geochemistry and genesis of the angrites. Geochimica et Cosmochimica Acta, 54, 3209–3218.

Miyamoto, M., and Takeda, H. (1994) Evidence for excavation of deep crustal material of a Vesta-like body from Ca compositional gradients in pyroxene. Earth and Planetary Science Letters, 122, 343–349.

Ohsumi, K., Hagiya, K., and Ohmasa, M. (1991) Development of a sys-

tem to analyze the structure of a submicrometer-sized single crystal by synchrotron X-ray diffraction. Journal of Applied Crystallography, 24, 340–348.

Ohsumi, K., Miyamoto, M., and Takase, T. (1993) Diffraction study of olivines in thin sections by micro-region Laue method using synchrotron radiation. Abstract for 18th Symposium on Antarctic Meteorites, 18, 192–194.

Ohsumi, K., Miyamoto, M., Takase, T., Kojima, H., and Yanai, K. (1994) Diffraction profile analysis of olivines in thin sections of meteorites by the micro-region Laue method using synchrotron radiation. Proceedings of NIPR Symposium on Antarctic Meteorites, 7, 244–251.

Petaev, M.I., and Brearley, A.J. (1994) Lamellar olivine in the Divnoe achondrite: EPMA and TEM studies. Lunar and Planetary Science, XXV, 1069–1070.

Petaev, M.I., Barsukova, L.D., Lipschutz, M.E., Wang, M.-S., Ariskin, A.A., Clayton, R.N., and Mayeda, T.K. (1994) The Divnoe achondrite: Petrology, chemistry, oxygen isotopes and origin. Meteoritics, 29, 182–199.

Prinz, M., Keil, K., Hlava, P.F., Berkley, J.L. Gomes, C.B., Cuvello, W.S. (1977) Studies of Brazilian meteorites: III. Origin and history of the Angra dos Reis achondrite. Earth and Planetary Science Letters, 35, 317–330.

Prinz, M., Weisberg, M.K., and Nehru, C.E. (1988) LEW 86010, a second angrite: Relationship to CAI's and opaque matrix. Lunar and Planetary Science, XIX, 949–950.

Putnis, A. (1992) Introduction to mineral sciences, 457 p. Cambridge University Press, Cambridge, U.K.

Sahama, T.G., and Hytönen, K. (1957) Kirschsteinite, a natural analogue to synthetic iron monticellite, from the Belgian Congo. Mineralogical Magazine, 31, 698.

——— (1958) Calcium-bearing magnesium-iron olivines. American Mineralogist, 43, 862–871.

Tracy, R.J., Jaffe, H.W., and Robinson, P. (1978) Monticellite marble at Cascade Mountain, Adirondack Mountains, New York. American Mineralogist, 63, 991–999.

Willemse, J., and Bensch, J.J. (1964) Inclusions of original carbonate rocks in gabbro and norite of the eastern part of the Bushveld Complex. Transactions of the Geological Society of South Africa, 67, 1–87.

Yanai, K. (1991) Olivine fassaite basalt: An unusual achondrite from Antarctica. Lunar and Planetary Science, XXII, 1539–1540.

Manuscript received August 9, 1994
Manuscript accepted January 11, 1995